An Experimental Study for Estimating the Effect of Compressive Axial Force on Seismic Performance of Steel Members

Kiyoshi ONO[1], Seiji OKADA[2], Nobuo NISHIMURA[3] and Nobuyuki HATTORI[4]

Abstract

Some methods of evaluating the seismic performance of hollow steel bridge piers have been already proposed in the previous investigations. Almost previous studies dealt with steel piers and members subject to relatively low compressive axial force that is below $0.2N_y$, where N_y is yield axial force. Little is known about the seismic performance of steel members subject to the compressive axial force that exceeds $0.2N_y$. On the other hand, it is reported that the huge earthquakes like the Hyogo-ken Nanbu earthquake may cause the high compressive axial force in the steel members such as arch ribs and towers of suspension bridges. Therefore, it is very important to grasp the seismic performance of steel members under the high compressive axial force in order to develop the seismic design method of them.

In this study, cyclic loading experiments are conducted by changing the value of the compressive axial force applied to each test specimen. On the basis of the experimental results, the effect of the compressive axial force on the seismic performance of steel members is investigated.

1 INTRODUCTION

The Hyogo-ken Nanbu Earthquake occurred in January 1995, and it caused destructive damages to highway bridges like never seen before in Japan. The damages such as buckling of stiffened plates, fracture of welding and large residual displacements of steel bridge piers were observed. The damage included the collapse of two rectangular cross section steel bridge piers[1)]. The earthquake provided a large impact on the earthquake disaster prevention measures in various fields and revealed that there are a lot of critical issues to be revised in seismic design. The specifications for highway bridges were revised in 1996[2),3)] in consideration of the damage and the ductility design method, which had already been adapted to reinforced concrete bridge piers, was also introduced to steel bridges. And the more detailed seismic design method for steel bridge piers is specified in the 2002 specifications[4),5)]. Besides the specifications for highway bridges, some methods for estimating the seismic performance of steel bridge piers or steel members have been already proposed[6)].

By the way, it is reported that the huge earthquakes like the Hyogo-ken Nanbu earthquake may cause the high compressive axial force in the steel members such as arch ribs and towers of suspension bridges by varying axial force and there are some cases that the compressive axial force exceeds $0.5N_y$[7)]. Here, N_y represents the yield axial force. However, the previous methods mentioned above were proposed on the basis of the researches as to steel bridge piers and steel members subject to the compressive axial force whose value is below $0.2N_y$[8)] and few researches were made on steel members under high compressive axial force such as $0.5N_y$.

[1] Associate Professor, Department of Civil Engineering, Osaka University
[2] Bridge Design Department, Ishikawajima-Harima Heavy Industries Co., Ltd.
[3] Professor, Department of Civil Engineering, Osaka University
[4] Student in Master Curse, Department of Civil Engineering, Osaka University

Table 1 Parameters of Test Specimens

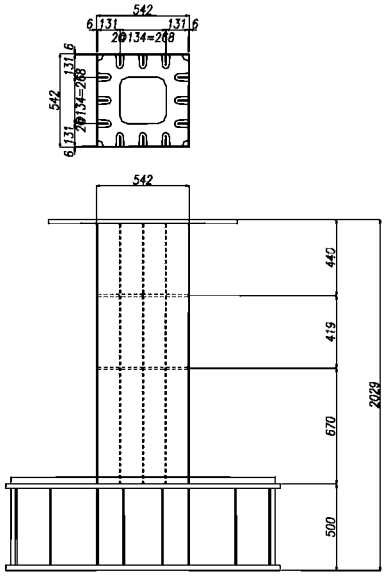

Fig. 1 Test Specimen

		N0.15	N0.35	N0.50
The size of cross-section (mm)		542 X 542	542 X 542	542 X 542
Thickness of flange plate tF (mm)		6	6	6
Thickness of web plate tW (mm)		6	6	6
The size of longitudinal stiffener (mm)		60 X 6	60 X 6	60 X 6
The number of stiffeners on flange		3	3	3
The number of stiffeners on web		3	3	3
Area (cm^2)		172	172	172
Moment of inertia (cm^4)		76,184	76,184	76,184
Compressive Axial Force (kN)		808	1,886	2,694
The height of Loading point (mm)		1,779	1,779	1,779
Steel grade (JIS)		SM490A	SM490A	SM490A
γ/γ^*		1.18	1.18	1.18
Parameters calculated by nominal yield stress σ_{yN}	$\bar{\lambda}$	0.21	0.21	0.21
	R_R	0.46	0.46	0.46
	R_F	0.43	0.43	0.43
	R_S	0.63	0.63	0.63
Parameters calculated by experimental yield stress σ_{yM}	σ_y(MPa)	397	397	397
	$\bar{\lambda}$	0.24	0.24	0.24
	R_R	0.52	0.52	0.52
	R_F	0.48	0.48	0.48
	R_S	0.70	0.70	0.70

So it is not clear that the previous methods can be applied to the steel members subject to the high compressive axial force. It is necessary to grasp the effect of the compressive axial force on the seismic performance of steel members for estimating the seismic performance of steel members under the high compressive axial force. The certain way is to take hold of the seismic performance by means of experiments.

In this study, cyclic loading experiments are conducted by changing the value of compressive axial force applied to each test specimen. On the basis of the experimental results, the effect of the compressive axial force on the seismic performance of steel members is investigated.

2 OUTLINE OF EXPERIMENTS

2.1 Test Specimens

In this investigation, three test specimens were employed. The values of the compressive axial force applied to each specimen were different. The figures in the name of each test specimens, 0.15, 0.35, 0.50 in Table 1 express the ratio of each compressive axial force to the yield axial force, N/N_{yN}. Here, N_{yN} is the yield axial force calculated by the following equation.

$$N_{yN} = \sigma_{y_N} \times A \tag{1}$$

Where σ_{yN} = nominal yield stress; A =sectional area.

The dimension, steel grade, and distribution of stiffeners of three test specimens were same. The outline of the dimensions of test specimen is given in Fig.1 and the values of major parameters of the test specimens are listed in Table 1. In Table 1, R_R, R_F and R_S are the

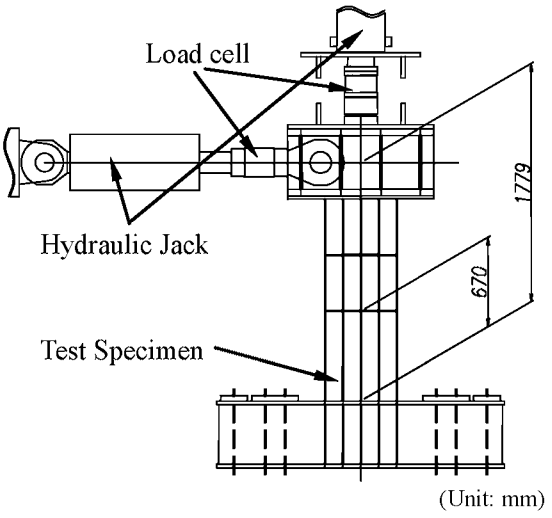

Fig. 2 Test Setup

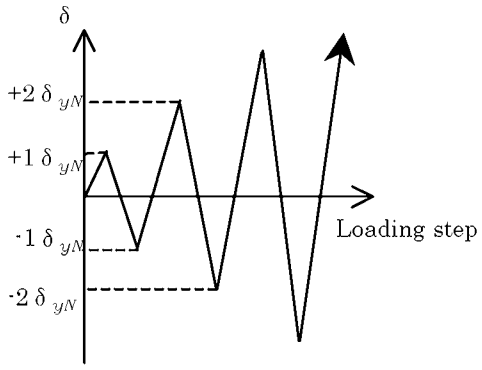

Fig. 3 Cyclic Pattern of Horizontal Load

buckling parameters of plate panels between longitudinal stiffeners, stiffened plate panels and longitudinal stiffeners respectively. $\overline{\lambda}$ is a slenderness ratio parameter of the column. The definitions of parameters mentioned above are identical to those stipulated in the 2002 specifications[4] and given as follows.

$$\overline{\lambda} = \frac{1}{\pi}\sqrt{\frac{\sigma_{yM}}{E}}\frac{l}{r} \tag{2}$$

$$R_R = \frac{b}{t}\sqrt{\frac{\sigma_{yM}}{E}\frac{12\left(1-\nu^2\right)}{4\pi^2 n^2}} \tag{3}$$

$$R_F = \frac{b}{t}\sqrt{\frac{\sigma_{yM}}{E}\frac{12\left(1-\nu^2\right)}{\pi^2 k_F}} \tag{4}$$

$$R_S = \frac{b}{t}\sqrt{\frac{\sigma_{yM}}{E}\frac{12\left(1-\nu^2\right)}{0.43\pi^2}} \tag{5}$$

where l = column height (distance from the bottom of the column to the point of application of horizontal load); r = radius of gyration of cross section; σ_{yM}= yield stress gained from material experiment; E = Young's modulus; b = flange width; t = plate thickness; ν = Poisson's ratio; n = number of panels; k_R = bucking coefficient.

The steel grade of test specimens was SM490. In all specimens, the plate thickness of webs, flanges and stiffeners was 6 mm.

2.2 Cyclic Program

Fig.2 is an outline of test setup. Each specimen was loaded with hydraulic jacks installed in a fully stiff frame. In respective experiment, the specified compressive axial force as shown in Table 1 was first applied to the specimen by the vertical hydraulic jack. The values of

compressive axial force, N, applied to each test specimen were 15%, 35% and 50% of yield axial force, N_{yN}, calculated by the equation (1).

The cyclic pattern of the horizontal displacement is schematically shown in Fig. 3, where δ_{yN} is the yield horizontal displacement calculated by the following equations. The compressive axial load was kept constant during each cyclic experiment.

$$P_{yN} = \left(\sigma_{yN} - \frac{N}{A} \right) \frac{Z}{l} \tag{6}$$

$$\delta_{yN} = \frac{P_{yN} l^3}{3EI} \tag{7}$$

Where Z = section modulus.

3 EXPERIMENTAL RESULTS AND COMMENTS

3.1 Feature of hysteretic curves

Fig.4 shows horizontal load – horizontal displacement hysteretic curves and Fig.5 shows the envelope curves of the hysteretic curves. The major values of experimental results are shown in Table 2. Definitions of symbols in Table 2 are illustrated in Fig.6 and explanations of them are described as follows. P_{max} is the maximum horizontal load. δ_m is the horizontal displacement at P_{max}. P_{yM} is the yield horizontal load calculated by equation (6) with σ_{yM} instead of σ_{yN}. δ_{yM} is the yield horizontal displacement at P_{yM} calculated by Timoshenko beam theory and δ_{yEM} is yield horizontal displacement at P_{yM} by using the initial stiffness obtained from the experimental results. N_{yM} is yield axial force calculated by the equation (1) with σ_{yM} instead of σ_{yN}. The square symbols (◆) in Fig.5 show the points where P_{max} occurred.

Fig.4 shows that the hysteretic loop size, P_{max} and δ_m decrease with the increase in the compressive axial force. The same tendency can be observed in envelop curves in Fig.5. Fig.5 exhibits that the increase of the compressive axial force makes slope of envelop curves after P_{max} steep. The feature of hysteric curves mentioned above is not good in terms of seismic performance.

3.2 Buckling Modes

Fig.7 shows the buckling modes of stiffened plates of the base sections and Fig.8 shows the residual deformations of flange panels of base sections after experiments. In Fig.8, positive values mean the out-of-plane deformations occurred outside of test specimens. As for test specimens N0.15 and N0.35, the local bucking concentrated near the bottom of the base section. The buckling modes of test specimens N0.15 and N0.35 were the typical buckling modes observed in test specimens with similar buckling parameters to those of test specimens N0.15 and N0.35 in the previous studies. On the other hand, for test specimen N0.50, not only the local buckling near the bottom but also the overall buckling of stiffened plates of base section was observed and the deformations of the overall buckling were larger than those of the local buckling. It is thought that the buckling modes were influenced by the ratio of the bending moment to the compressive axial force which acted on the base sections. Fig.9 expresses the progress of out-of-plan deformations of flange panels at points shown in Fig.10.

The dotted lines in Fig.9 correspond to the loops where P_{max} occurred in the experiments. Fig.9 exhibits that the out-of-plan deformations developed rapidly after P_{max} for all test specimens. By the way, maximum deformation of test specimen N0.50 shown in Fig.9 was smaller than those of test specimens N0.15 and N0.35. The cause of this small deformation is that the points where out-of-plane deformations were measured were not near the point where maximum deformation occurred in test specimen N0.50.

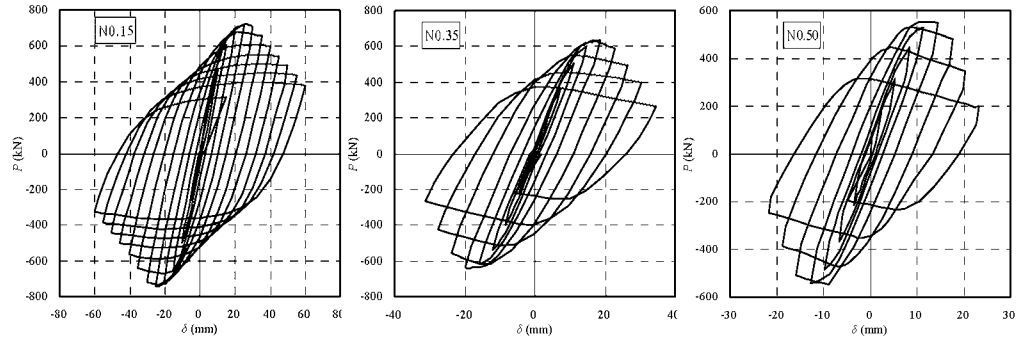

Fig. 4 Hysteretic Curves

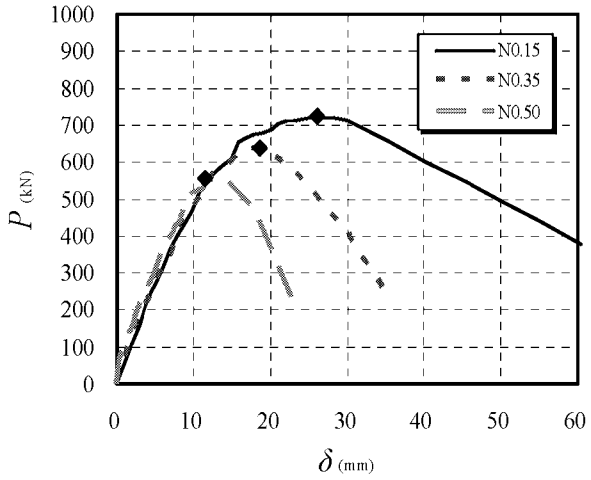

Fig. 5 Envelope Curve

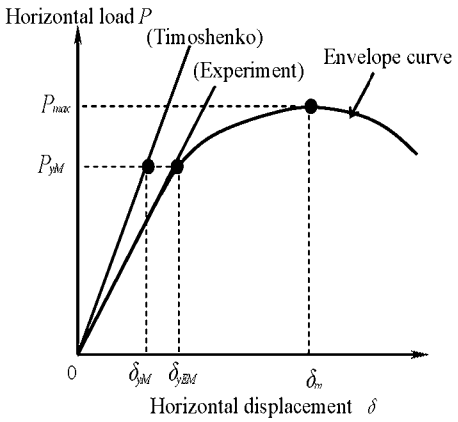

Fig. 6 Definition of Symbol

Table 2 Experimental Results

Specimen	N0.15	N0.35	N0.50
N/N_{yM}	0.12	0.28	0.39
P_{yM} (kN)	553	454	380
P_{max} (kN)	723	637	554
P_{max}/P_{yM}	1.31	1.40	1.46
δ_{yM} (mm)	8.2	6.7	5.6
δ_{yEM} (mm)	11.4	9.7	7.3
δ_m (mm)	26.0	18.6	11.5
δ_m/δ_{yEM}	2.28	1.93	1.58

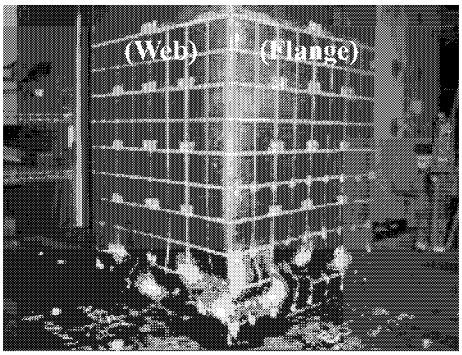

(N0.15)

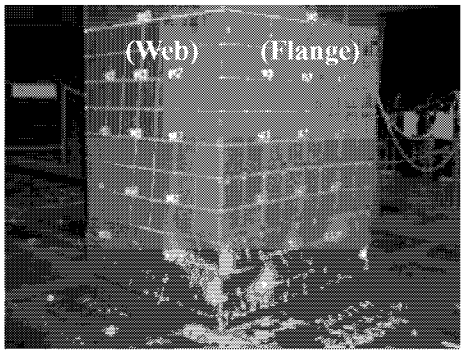

(N0.35)

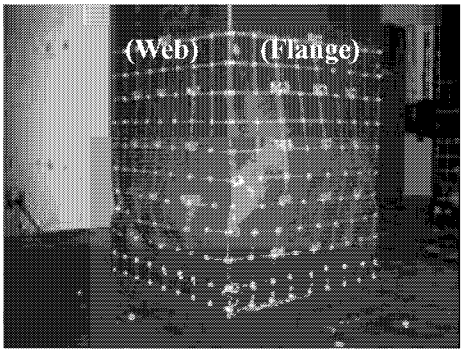

(N0.50)

Fig.7 Buckling Modes

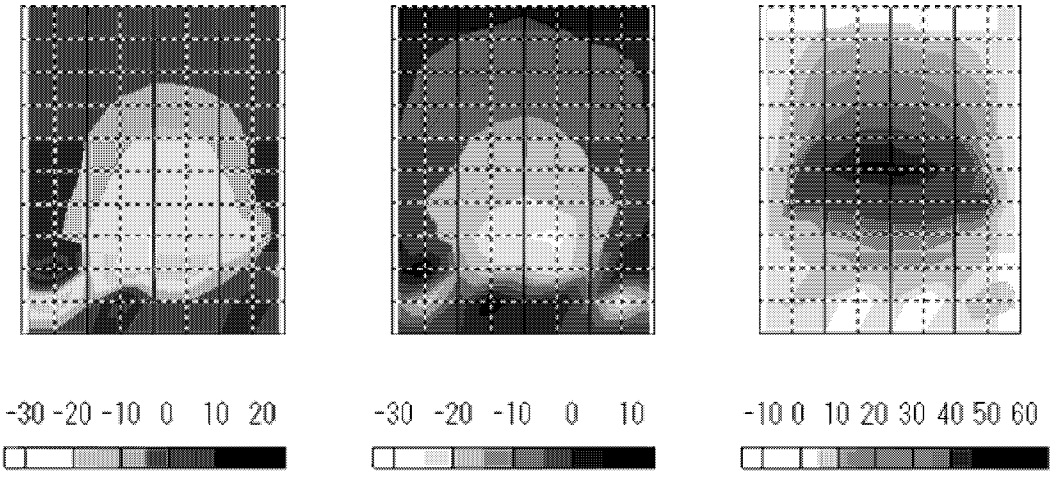

(N0.15) (N0.35) (N0.50)

(unit: mm)

Fig. 8 Residual Deformation of Flange

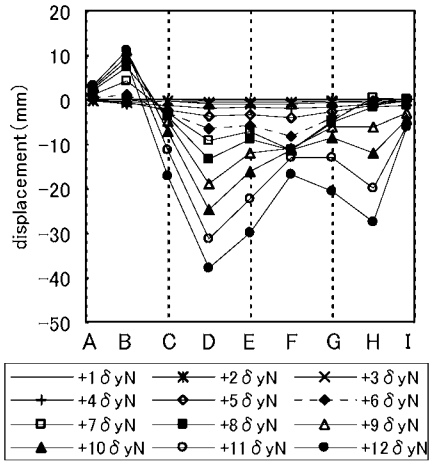

(N0.15)

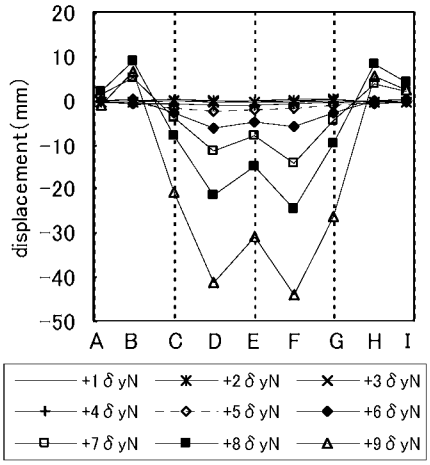

(N0.35)

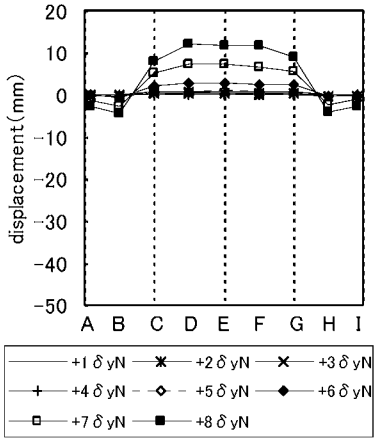

(N0.50)

Fig. 9 Progress of out-of-plane deformation of Flange

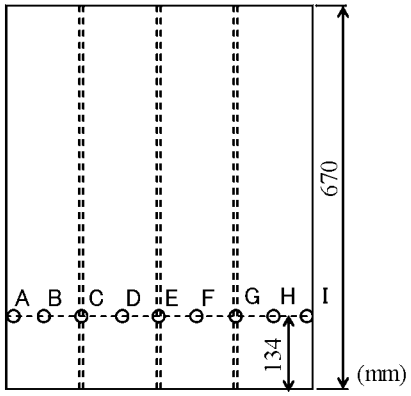

Fig. 10 Measuring Points

4 CONCLUSION

Cyclic loading experiments were conducted by changing the value of compressive axial force applied to three test specimens in order to gasp the effect of the compressive axial force on seismic performance of steel members. The results from experiments are concluded as follows.

1) The increase in the compressive axial force caused the decrease in the hysteretic loop size, the maximum horizontal load and the horizontal displacement at the maximum horizontal load and it made slope of envelop curves after the maximum horizontal load steep. The feature of hysteretic curves mentioned above is not good in terms of seismic performance.
2) The buckling modes of the test specimen subject to the high compressive axial force such as $0.5N_{yN}$ were different from those of other test specimens. It is thought the buckling modes were influenced by the ratio of the bending moment to the compressive axial force which acted on the base sections.

ACKNOWLEDGMENTS

The experiments in this paper were curried out as a collaboration between Osaka University and Ishikawajima-Harima Heavy Industries Co., Ltd.. The authors wish to express appreciation toward participants in this collaboration.

REFERENCES

1) Ministry of Construction: Report on the damage of Highway Bridges by the Hyog-ken Nanbu Earthquake, Committee for Investigation on the Damage of Highway Bridges caused by the Hyogo-ken Nanbu Earthquake, 1995 (in Japanese).
2) Japan Road Association: Specification for highway bridges, Part II ; Steel Bridges , 1996(in Japanese).
3) Japan Road Association: Specification for highway bridges, Part V; Seismic Design, 1996(in Japanese).
4) Japan Road Association: Specification for highway bridges, Part II ; Steel Bridges , 2002(in Japanese).
5) Japan Road Association: Specification for highway bridges, Part V; Seismic Design, 2002(in Japanese).
6) Usami, T. and Oda H.: Numerical analysis and verification methods for seismic design steel structures, J. Struct. Mech. / Earthquake Eng., JSCE, Vol.668/ I -54, pp.1-15, 2001(in Japanese).
7) Nonaka, T., Usami, T., Yoshino, H, Sakamoto, Y. and Torigoe, T.: Elastic-plastic behavior and improvement of seismic performance for upper-deck type steel arch bridges, J. Struct. Mech. / Earthquake Eng., JSCE, Vol.731/ I -63, pp.31-50, 2003(in Japanese).
8) Public Works Research Institute of the Ministry of Construction and five other organizations (PWRI et al.); Ultimate Limit State Design Method of Highway Bridges Piers under Seismic Loading, Cooperative Research Report, 1997-1999(in Japanese).